

Effects of Control Power and Guidance Cues on Lunar Lander Handling Qualities

Karl D. Bilimoria*

NASA Ames Research Center, Moffett Field, California 94035

DOI: 10.2514/1.40187

A piloted simulation was conducted to study handling qualities for a precision lunar landing task from final approach to touchdown. The experiment variables were control power and guidance cues. A dynamics and control model was derived from Apollo Lunar Module data, and new feedback guidance laws were designed to help the pilot follow a reference trajectory. The experiment was conducted on the large motion base Vertical Motion Simulator at the NASA Ames Research Center. Six pilot astronauts served as evaluation pilots, providing Cooper–Harper ratings, Task Load Index ratings, and qualitative comments. The piloting task was to fly a final approach profile from 500 ft altitude located 1350 ft up range of the designated landing site with a 250 ft lateral offset, and touch down with a position accuracy of 15 ft. Following guidance cues presented on cockpit displays, the pilots were able to accomplish this task for control powers ranging from 100 to 15% of the nominal (Apollo) value. The handling qualities were satisfactory (Level 1) at nominal control power, and degraded nonlinearly as control power decreased. Without guidance cues, in the limited time available for this experiment, the evaluation pilots were unable to develop a flying technique for the precision landing task with lateral offset approach. This highlights the need for guidance cues in future lunar operations that may require precision landing capability.

Nomenclature

a	=	translational acceleration, ft/s^2
\mathcal{F}	=	thrust of a Reaction Control System jet, lb
g_{lunar}	=	gravitational acceleration at lunar surface, ft/s^2
h	=	height above lunar surface, ft
\dot{h}	=	time derivative of h , ft/s
$I_{(0)}$	=	moment of inertia, $\text{slug} \cdot \text{ft}^2$
K	=	feedback gain
k	=	parameter for tradeoff between propellant consumption and error settling time
ℓ	=	moment arm from Reaction Control System jet to vehicle center of mass, ft
M	=	moment about vehicle center of mass due to thrust of a Reaction Control System jet, $\text{ft} \cdot \text{lb}$
m	=	vehicle mass, slug
p	=	roll rate, deg /s
q	=	pitch rate, deg /s
r	=	yaw rate, deg /s
R	=	range from landing site, ft
\dot{R}	=	time derivative of R , ft/s
T	=	thrust of descent engine, lb
T^o	=	value of T required for vertical force equilibrium, lb
t	=	time, s
V	=	vehicle velocity over lunar surface, ft/s
x, y	=	position coordinates, ft
α	=	nominal angular acceleration, deg / s^2
θ	=	pitch angle, deg
τ	=	time constant, s
ϕ	=	roll angle, deg
ψ	=	yaw angle, deg

Subscripts

cmd	=	commanded value
D	=	down component
DB	=	deadband
E	=	east component
err	=	error value
horiz	=	component in the horizontal plane
N	=	north component
X, Y	=	components along vehicle body x, y axis

Superscripts

$*$	=	along reference trajectory
G	=	guidance value
ROD	=	rate of descent

Introduction

HANDLING qualities are those characteristics of a flight vehicle that govern the ease and precision with which a pilot is able to perform a flying task [1]. They are a manifestation of the interaction between various factors that influence pilot perception of how well (or poorly) a vehicle can be flown to accomplish a desired mission. These factors include the stability and control characteristics of the bare vehicle, the control systems that enhance these characteristics, the inceptors (e.g., control column or throttle lever) used by the pilot to transmit control commands, the visual cues from cockpit windows and displays/instrumentation that provide flight information to the pilot, and other cues (e.g., aural, tactile) that assist the pilot in the execution of the flying task.

The handling qualities of aircraft have been extensively studied over several decades [2–6]. Reference standards for the handling qualities of both fixed-wing aircraft [7] and rotary-wing aircraft [8] have been developed, and are now in common use. Broadly speaking, these standards define a subset of the dynamics/control design space that provides good handling qualities for a given vehicle type and flying task. For example, the standards may specify a range of combinations of damping and natural frequency for a large aircraft during landing.

At this time, no reference standards exist for spacecraft handling qualities. However, there is a modest body of work on handling qualities of piloted spacecraft. Powers [9] covered space shuttle landing, although the use of aerodynamic controls for this flight

Presented as Paper 7799 at the AIAA SPACE 2008 Conference & Exposition, San Diego, CA, 9–11 September 2008; received 31 July 2008; revision received 22 July 2009; accepted for publication 2 August 2009. This material is declared a work of the U.S. Government and is not subject to copyright protection in the United States. Copies of this paper may be made for personal or internal use, on condition that the copier pay the \$10.00 per-copy fee to the Copyright Clearance Center, Inc., 222 Rosewood Drive, Danvers, MA 01923; include the code 0022-4650/09 and \$10.00 in correspondence with the CCC.

*Research Scientist, Flight Trajectory Dynamics and Controls Branch, Mail Stop 210-10; Karl.Bilimoria@nasa.gov. Associate Fellow AIAA.

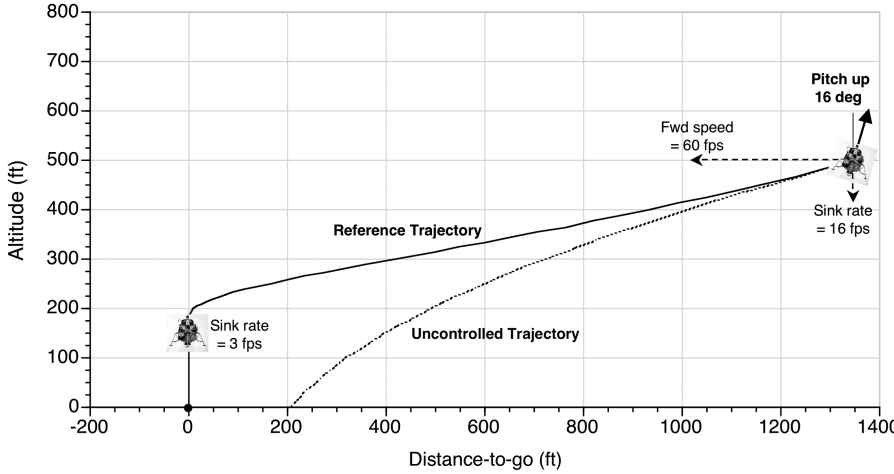


Fig. 1 Reference trajectory profile in the vertical plane.

phase makes it aircraftlike. Exoatmospheric attitude control of spacecraft generally uses reaction control jet thrusters, and Besco [10] reported a study on the relationship between attitude-control response type and handling qualities for piloted spacecraft. A large portion of the existing literature on spacecraft handling qualities pertains to the Apollo Lunar Module [11–20]. These handling qualities studies were conducted using fixed-base simulators, the Lunar Landing Research Facility [21], which featured a test vehicle suspended from a traveling crane moving along a large gantry structure, and the free-flying Lunar Landing Research Vehicle [22].

A new generation of piloted spacecraft is now being designed [23]. The ability of pilots to successfully carry out their missions will be determined in part by the handling qualities of these new spacecraft. Some flight operations may be fully automated, whereas others may be executed with a human pilot engaged in various levels of supervisory control including manual flying tasks [24]. It is noted that current NASA procedures require that human-rated spacecraft provide the capability for the crew to manually control the flight path and attitude with satisfactory handling qualities [25]. Even for flight operations that are nominally executed in a highly automated control mode, the control architecture must provide the capability for a human pilot to switch to a manual control mode, whether due to failure of an automated system or of some component of the spacecraft. In these cases of emergency reversion to manual control, in which the pilot role abruptly switches from monitoring to active control, it is important that the vehicle have acceptable handling qualities. It is therefore desirable for spacecraft designers to assess early in the design cycle what the handling qualities will likely be, and to adjust their design if necessary to ensure that adequate handling qualities are preserved even in degraded or failed operational modes.

An effort to develop design guidelines for spacecraft handling qualities was initiated by NASA in 2007. A comprehensive set of guidelines should cover all classes of spacecraft and phases of flight; however, near-term NASA program goals make it necessary to focus initially on a few specific and relevant aspects. Two recent experiments investigating the handling qualities of spacecraft docking in low Earth orbit are described in [26,27].

This paper reports an experiment investigating the final approach and terminal descent phases of lunar landing, which present a particularly challenging flying task. In an interview, Neil Armstrong said: “The most difficult part from my perspective, and the one that gave me the most pause, was the final descent to landing. That was far and away the most complex part of the flight. . . . I thought that the lunar descent on a ten scale was probably a 13.”[†]

In the Apollo lunar missions, it was sufficient to land within several hundred feet of the designated landing site. Future lunar outpost missions may require precision landing capability at designated sites for logistical reasons. This work investigates the handling qualities for a precision lunar landing task from final approach to touchdown, for various control powers, with and without guidance cues. The following section describes the experiment design. The next section presents the dynamics/control model derived from Apollo Lunar Lander data as well as the precision landing guidance laws developed for this work; it is followed by a section describing the simulation environment. Results from a piloted simulation are then presented, followed by conclusions.

Experiment Design

A piloted evaluation of lunar lander handling qualities was conducted in May–June 2007 at the NASA Ames Research Center. This section describes various aspects of the experiment design.

Flying Task

This experiment evaluated handling qualities for a precision landing task, from final approach through terminal descent to touchdown. Coarse trajectory changes were made by firing opposing Reaction Control System (RCS) jets to change the attitude of the lander and hence tilt the descent engine’s thrust vector. In a near-level attitude, fine trajectory changes could be made by firing RCS jets in the same direction. Feedback guidance laws were developed for flying the precision landing task, and the corresponding guidance cues were displayed to the pilot via cockpit instrumentation. Details of the dynamics and control model are presented in the next section.

The task began at 500 ft (152.4 m) altitude with a forward speed of 60 fps (18.3 m/s) and a descent rate of 16 fps (4.9 m/s); for Apollo missions this was known as “low gate” and represented the point on the trajectory at which the manual flying phase would begin. At this point, the spacecraft was at 1350 ft (411.5 m) range from the designated touchdown point, and pitched up 16 deg. The desired trajectory brought the spacecraft to a level attitude directly above the touchdown point, at an altitude of 150 ft (45.7 m) with a descent rate of 3 fps (0.9 m/s). This rate of descent was held constant until one of the 6 ft (1.8 m) probes attached to the lander legs made contact with the lunar surface. A shutoff command was then sent to the main engine, and the vehicle dropped until the legs settled on the lunar surface. This reference trajectory profile is illustrated in Fig. 1. For comparison, it also shows the uncontrolled trajectory that would result if no pilot inputs were made starting from an initial condition with vertical force equilibrium.

The dynamics of the trajectory described here are confined to the vertical plane, with pitch attitude as the primary means of longitudinal trajectory control. To excite lateral dynamics, the initial

[†]More data about the 19 Sept. 2001 oral history transcript from the NASA Johnson Space Center Oral History Project available online at www.nasa.gov/pdf/62281main_armstrong_oralhistory.pdf [retrieved 25 July 2008].

condition was given a lateral offset of 250 ft (76.2 m) from the touchdown point so that the initial velocity vector did not point directly at the landing site, requiring the use of roll attitude as the primary means of lateral trajectory control.

Experiment Matrix

The objective of this experiment was to evaluate the effects of control power and guidance cues on handling qualities for a precision lunar landing task. Control power refers to the RCS jet thrust, which directly affects angular acceleration for opposing jet firings and translational acceleration for same-direction firings. Six values of control power ranging from 100 to 15% of the nominal Apollo Lunar Module value were selected for evaluation, based on trial runs with development pilots before the experiment. The primary goal of the experiment was to assess the variation of handling qualities with control power. A secondary goal was to assess handling qualities with and without guidance cues. The experiment matrix is depicted in Fig. 2.

The original experiment plan was to conduct handling qualities assessments for a lateral offset approach with guidance on and off. However, it was found that the precision landing task with offset approach and guidance off was extremely difficult, and the pilots were unable to develop a flying technique for this two-axis-control task in the limited time available. A centerline approach (zero lateral offset) was flyable with guidance off, and this single-axis-control task was substituted in the experiment matrix. It should be noted that a direct comparison of guidance on/off cases cannot be made now, because the two flying tasks are quite different.

Evaluation Pilots

Six active-duty pilot astronauts from the NASA Johnson Space Center served as evaluation pilots. All were male and had substantial training/experience as test pilots before astronaut selection. They had logged an average of about 5000 h on various types of aircraft, and each had received many years of pilot astronaut training. Each pilot was available to the experimenters for about 8 h, and this time constraint was incorporated into the experiment design.

Training Procedures

Upon arrival, the pilot received a detailed briefing on the experiment background and objectives, flying task, control system, experiment matrix, and data collection procedures. Including discussion time, this session lasted approximately 1 h. This was followed by a 1 h training and familiarization session in the simulator cockpit, where the pilot practiced the flying task for various control powers with guidance on as well as off, until he felt comfortable that most of the learning curve was behind him.

Data Collection Procedures

Each pilot encountered the six control powers in a randomized sequence and was not told the value of the control power. Pilots first flew all configurations for offset approach with guidance on, and then flew all configurations for centerline approach with guidance off. For each test configuration (e.g., offset approach with guidance on and 100% control power), the pilot flew three consecutive data collection runs, and then provided experiment data for that test configuration as described below.

Control Power →	15%	20%	25%	30%	50%	100% (Apollo)
Guidance Cues ↓	ON Offset Approach					
	OFF Centerline Approach					

Fig. 2 Experiment matrix.

In handling qualities experiments, pilots are generally asked to make a composite assessment of the overall performance across all data collection runs for a test configuration. It is important to note that this assessment takes into account not just the quantitative evaluation of the end point (e.g., touchdown) performance but also a qualitative evaluation of the manner in which the vehicle gets to the end point. This overall assessment of desired, adequate, or inadequate performance is used for walking through the decision tree in the Cooper–Harper chart [1]. Pilots use the Cooper–Harper scale to assign handling qualities ratings from 1 (best) to 10 (worst) based on their assessment of task performance and effort. It is an ordinal scale, which means, for example, that the difference between ratings of 1 and 2 is not the same as the difference between ratings of 3 and 4. Ratings of 1, 2, and 3 on the Cooper–Harper scale correspond to Level 1 handling qualities, which are a general requirement for normal operations of flight vehicles. Ratings of 4, 5, and 6 correspond to Level 2, which may be acceptable for some off-nominal conditions, and ratings of 7, 8, and 9 correspond to Level 3, which is acceptable only for transition to a safe mode after a major failure/disturbance. Desired performance is necessary (but not sufficient) for Level 1 ratings, and adequate performance is necessary (but not sufficient) for Level 2 ratings. It is noted that Apollo-era studies [11–20] on Lunar Module handling qualities used the Cooper rating scale [1], which was a precursor of, and quite different from, the Cooper–Harper rating scale used in this work.

At the end of each run, relevant touchdown performance parameters (see Fig. 3) were displayed to the pilot and experimenter; values outside the adequate performance bounds were colored-coded red. The values of adequate performance bounds for key parameters were obtained from a survey of Apollo Lunar Module literature; the 15 ft (4.6 m) range error limit for this precision landing task was obtained as half of the diagonal distance between the lander legs. It is noted that there were no specified values for desired performance bounds. These values should ideally be determined by working with development pilots before the experiment, but are sometimes specified simply as a fraction (e.g., half) of the adequate values. In this experiment, the evaluation pilots were asked to make their own assessment of desired touchdown performance.

After making a composite assessment of the overall performance across the three data collection runs for a test configuration, pilots walked through the Cooper–Harper chart and assigned a handling qualities rating for that test configuration. Next, they assigned ratings for each of the six components of the NASA Task Load Index [28]. These six components were physical demand, mental demand, temporal demand, performance, effort, and frustration. As appropriate, pilots also made qualitative comments about the test configuration they had just evaluated. All pilot comments were recorded on electronic media; the experimenter noted key points.

After all test configurations had been evaluated, there was a debrief session. The pilots were asked to fill out a one-page questionnaire designed to elicit high-level comments on cockpit displays, out-the-window displays, guidance cues, control response, and experiment design. This was followed by a discussion with the experimenter.

Limits of Touchdown Values	
Roll Angle ± 6 deg	Roll Rate ± 6 deg/s
Pitch Angle ± 6 deg	Pitch Rate ± 6 deg/s
Range 15 ft = 4.6 m	Yaw Rate ± 1.5 deg/s
Horizontal Speed 4 fps = 1.2 m/s	Descent Rate 8 fps = 2.4 m/s
Descent Engine Fuel Burn 1500 lbm = 680 kg	RCS Jets Fuel Burn 150 lbm = 68 kg

Fig. 3 Limits of adequate touchdown performance.

Lunar Lander Dynamics and Control Model

Because NASA's Constellation program lunar lander [29] (currently named Altair) was still in the conceptual design stage when this study was initiated in January 2007, a generic model was created based on Apollo Lunar Module data gathered from various sources such as [30–32]. In the model used for this work, the lunar lander body axes system was a conventional aircraftlike system with origin at the c.m.; see schematic in Fig. 4.

Vehicle Mass/Inertia Model

The initial mass of the vehicle is 543 slugs (7925 kg); it then varies due to consumption of propellant by the descent engine and RCS jets. Moments of inertia along body axes are given by $I_{xx} = 16,099 \text{ slug} \cdot \text{ft}^2 = 21,827 \text{ kg} \cdot \text{m}^2$, $I_{yy} = 13,629 \text{ slug} \cdot \text{ft}^2 = 18,479 \text{ kg} \cdot \text{m}^2$, $I_{zz} = 12,750 \text{ slug} \cdot \text{ft}^2 = 17,287 \text{ kg} \cdot \text{m}^2$, $I_{xz} = -652 \text{ slug} \cdot \text{ft}^2 = -884 \text{ kg} \cdot \text{m}^2$, with I_{xy} and I_{yz} approximated by zero.

During the final approach to touchdown phase, the vehicle mass decreases by only 5% due to propellant consumption. Hence, in this model it is assumed that moments of inertia are constant and that the vehicle c.m. location remains constant.

Descent Engine

The descent engine is the spacecraft's main rocket engine, with a specific impulse of 311 s. For the landing task, its thrust force is used to regulate the descent rate and to apply coarse trajectory control in the horizontal plane by rolling and/or pitching the vehicle. In this model, the engine does not gimbal and the thrust line passes through the vehicle c.m. Propellant mass budgeted for the piloted segment of the landing trajectory, including reserves, is 50 slugs (730 kg).

The descent engine thrust is directed along the negative body z axis. During the flight phases from approach to touchdown, this thrust can be controlled by a throttle between 10 and 60% of the maximum value of 10,000 lb (44,482 N). The thrust command, T_{cmd} , consists of two parts. The primary part, T_{cmd}^o , is automatically computed as the force for which the vertical component balances the vehicle's lunar weight while compensating for vehicle roll (ϕ) and pitch (θ) angles.

$$T_{\text{cmd}}^o = \frac{mg_{\text{lunar}}}{\cos \phi \cos \theta} \quad (1)$$

The secondary part of the thrust command, ΔT_{cmd} , is an increment derived from pilot input. There are two modes for pilot input: a throttle increment mode and a rate-of-descent mode. In the throttle increment mode, each inceptor discrete input ("click") by the pilot increments the thrust by $\pm 1\%$ of the upper throttle limit value of 6000 lb. In the rate-of-descent mode, each inceptor click increments the commanded descent rate by $\pm 1 \text{ fpm}$ (0.3 m/s); the descent rate is regulated within a deadband of $\pm 0.1 \text{ fpm}$ (0.03 m/s) by a proportional feedback controller with a time constant $\tau = 1.5 \text{ s}$.

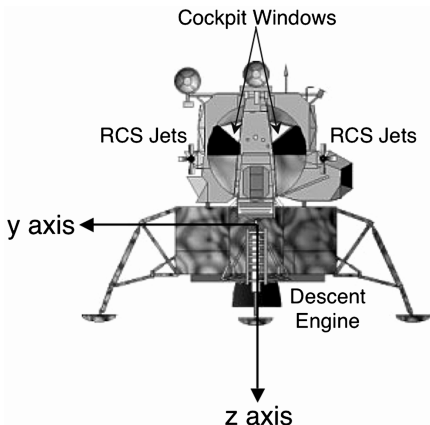


Fig. 4 Schematic of Apollo Lunar Module.

$$\Delta T_{\text{cmd}}^{\text{ROD}} = \frac{m}{\cos \phi \cos \theta} \left(\frac{\dot{h}_{\text{cmd}} - \dot{h}}{\tau} \right) \quad (2)$$

Engine response to thrust commands is modeled as a first-order system, with a time constant of 0.11 s. Hence, the actual thrust produced by the descent engine, T , lags the commanded thrust $T_{\text{cmd}} = T_{\text{cmd}}^o + \Delta T_{\text{cmd}}$.

Reaction Control System Jets

There are four clusters, each of which has four RCS jets with thrust axes oriented along the vehicle body axes. There are a total of 16 jets aligned as follows: eight jets along $\pm z$, four jets along $\pm y$, and four jets along $\pm x$. The RCS jet clusters are located at the corners of a square of length $2\ell = 11 \text{ ft}$ (3.4 m), located $\ell = 5.5 \text{ ft}$ (1.7 m) above the vehicle c.m. The nominal thrust of each jet, \mathcal{F} , is 100 lb (445 N), with a specific impulse of 290 s. The RCS jets cannot be throttled, and have fast response dynamics on the order of 10 ms. In this model, the response to an on/off command input is assumed to be instantaneous. Propellant mass budgeted for the piloted segment of the landing trajectory, including reserves, is 5 slugs (73 kg). RCS jets are used for three-axis attitude control; it is noted that roll/pitch attitude control provides indirect translation control in the horizontal plane. For the precision landing task, RCS jets can also be used for direct translation control in the horizontal plane when the vehicle is in a near-level attitude.

For direct translation control, two jets are fired in the same direction to create a force $2\mathcal{F} = 200 \text{ lb}$ (890 N) along the body x axis and/or y axis; note that these force(s) will generate pitch and/or roll moments due to the moment arm along the body z axis. It is noted that, during the powered descent phases of flight, RCS jets are not used to create translation-only forces along the body z axis.

For roll/pitch/yaw attitude control, two jets are fired in opposition to create a moment $2\mathcal{M} = 1100 \text{ ft} \cdot \text{lb}$ (1491 N · m), and there is no net force created. In the actual Apollo Lunar Module, the control logic would fire four jets to provide larger torques when angular rate errors exceeded a specified threshold [31]. However, due to the number and geometry of up/down firing jets, only two-jet torques were available simultaneously in the roll and pitch axes. In the experiment reported here, the four-jet torque feature is not used and two-jet torques are available in all three axes at all times.

In this work, selection and firing of individual jets are not modeled. The model simply uses aggregated forces/momenta that would be generated by the firing of various RCS jet combinations.

Direct Translation Control

Pilot inputs are made with a three-axis translation hand controller (THC); this control inceptor is used for fine control of the trajectory along the x and y body axes when the vehicle is in a near-level attitude. The control response type is acceleration command; this means that the appropriate RCS jets fire continuously to produce a constant acceleration for as long as the pilot holds the inceptor out of detent. For example, moving the THC forward will create a force of $2\mathcal{F}$ (and, hence, an acceleration of $2\mathcal{F}/m$) along the body x axis. Note that this will also create a nose-down pitching moment.

Attitude Control

By tilting the descent engine thrust vector, roll/pitch attitude control provides indirect translation control for coarse trajectory changes. Pilot inputs are made with a three-axis rotation hand controller (RHC); this control inceptor is used for attitude stabilization/control along all three body axes. The control response type is Rate Command Attitude Hold, implemented as described below.

Rate Command Mode

This mode is in effect along all three axes when the inceptor is out of detent in any axis. It is also in effect when the inceptor is in detent along all three axes and the sum of the absolute values of roll, pitch, and yaw rates is greater than or equal to 2 deg/s . The angular rate command is linearly proportional to the inceptor displacement with a

value of 20 deg/s at full inceptor deflection. Error signals are generated as the difference between the actual and desired angular rates:

$$\begin{Bmatrix} p_{\text{err}} \\ q_{\text{err}} \\ r_{\text{err}} \end{Bmatrix} = \begin{Bmatrix} p - p_{\text{cmd}} \\ q - q_{\text{cmd}} \\ r - r_{\text{cmd}} \end{Bmatrix} \quad (3)$$

where p, q, r are the roll, pitch, and yaw rates, respectively, along the vehicle body axes.

By firing RCS jets, control moments are generated about the appropriate axes until the attitude rate error signals are driven to zero within a rate deadband of 0.4 deg/s.

Attitude Hold Mode

This mode is in effect simultaneously along all three axes when the inceptor is in detent in all three axes, and the sum of the absolute values of roll, pitch, and yaw rates is less than 2 deg/s. In the Apollo Lunar Module, control moments were commanded about the appropriate axes based on phase-plane relationships between errors in angle and angular rate [31,32]. The same control approach is used in this work.

Error signals are given by

$$\begin{Bmatrix} p_{\text{err}} \\ q_{\text{err}} \\ r_{\text{err}} \end{Bmatrix} = \begin{Bmatrix} p \\ q \\ r \end{Bmatrix}$$

$$\begin{Bmatrix} \phi_{\text{err}} \\ \theta_{\text{err}} \\ \psi_{\text{err}} \end{Bmatrix} = \begin{bmatrix} 1 & 0 & -\sin \theta \\ 0 & \cos \phi & \sin \phi \cos \theta \\ 0 & -\sin \phi & \cos \phi \cos \theta \end{bmatrix} \begin{Bmatrix} \phi - \phi_{\text{hold}} \\ \theta - \theta_{\text{hold}} \\ \psi - \psi_{\text{hold}} \end{Bmatrix} \quad (4)$$

where (ϕ, θ, ψ) are the current values of the vehicle Euler angles, and $(\phi_{\text{hold}}, \theta_{\text{hold}}, \psi_{\text{hold}})$ are the Euler angle values captured when the attitude hold mode was last entered. Control moment commands are generated about the appropriate axes in accordance with the phase-plane relationship between error signals, as illustrated in Fig. 5 for the pitch axis. The two sets of switching curves depict the equalities:

$$\theta_{\text{err}} = \pm \left[\left(\frac{1}{2\alpha_p} \right) (q_{\text{err}})^2 - \theta_{\text{DB}} \right] \quad (5a)$$

$$\theta_{\text{err}} = \pm \left[\left(\frac{1}{2k\alpha_p} \right) (q_{\text{err}})^2 + \theta_{\text{DB}} \right] \quad (5b)$$

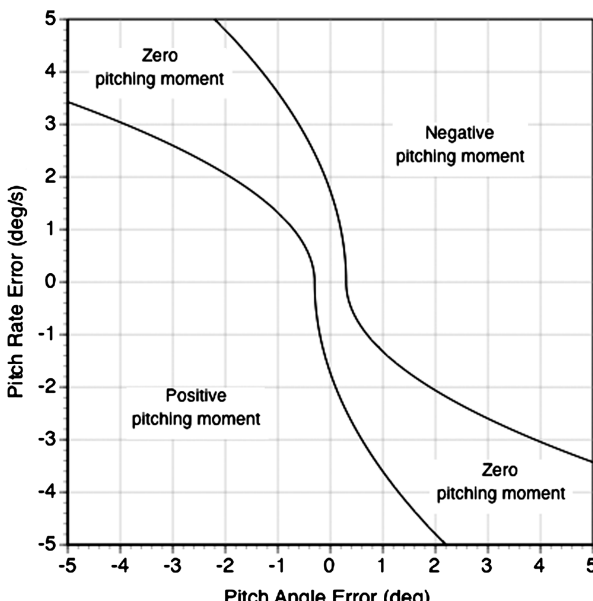


Fig. 5 Switching curves for pitch axis attitude hold.

where α_p is the nominal pitch acceleration approximated by $(2M/I_{yy}) = 4.5 \text{ deg/s}^2$, $\theta_{\text{DB}} = 0.3 \text{ deg}$ is the deadband for pitch attitude error, and $k = 0.25$ denotes a parameter that represents a tradeoff between RCS jet propellant consumption and error settling time.

Similar phase-plane relationships are defined for the roll and yaw axes, except for a small difference in the value of the nominal acceleration α in Eqs. (5a) and (5b); specifically, 4 deg/s² for roll and 5 deg/s² for yaw.

Guidance Laws

The Apollo lunar missions did not have a requirement for precision landing; it was sufficient to land within several hundred feet of the designated landing site. Therefore, the Apollo Lunar Module did not require, nor did it have, any active guidance cues displayed to the pilot for manual landing. The guidance laws presented herein were independently derived, and constitute one of the original contributions of this work. These laws were designed to guide the pilot along a reference trajectory (see Fig. 1) from final approach through terminal descent to lunar touchdown. In the equations presented next, time is in units of seconds and length is in units of feet. Variables along the reference trajectory are denoted by an asterisk superscript.

In the vertical dimension of the reference trajectory, the descent rate decreases linearly from 16 fps at 500 ft altitude to 3 fps at 150 ft altitude during the final approach phase, and then remains constant at 3 fps as the altitude decreases to zero during the terminal descent phase. Hence,

$$\dot{h}^* = (-0.03714h^* + 2.57) \quad \text{for } h^* \geq 150 \quad (6a)$$

$$\dot{h}^* = -3 \quad \text{for } h^* < 150 \quad (6b)$$

Noting that $h^*(0) = 500 \text{ ft}$, and analytically integrating Eq. (6a), we get

$$h^*(t) = 430.8 \exp(-0.03714t) + 69.2 \quad \text{for } h^* \geq 150 \quad (7)$$

Let Δt^* denote the time interval for the vehicle to descend along the reference trajectory from some altitude h^* to 150 ft altitude. From Eq. (7), we get

$$\Delta t^* = 26.93 \ln \left(\frac{h^* - 69.2}{80.8} \right) \quad (8)$$

In the horizontal dimension of the reference trajectory, the horizontal speed, V_{horiz}^* , at any range R from the landing site decreases to zero speed at zero range. Note that this needs to happen in the time Δt^* that it takes for the vehicle to descend to 150 ft altitude along the vertical dimension of the reference trajectory. The horizontal acceleration varies along the reference trajectory. However, for analytical convenience, let a_{horiz} represent an equivalent average acceleration in the horizontal plane over the time interval Δt^* . From kinematics, we have $a_{\text{horiz}} = -V_{\text{horiz}}^*/\Delta t^*$ and $R = V_{\text{horiz}}^* \Delta t^* + 0.5a_{\text{horiz}}(\Delta t^*)^2$; hence, $V_{\text{horiz}}^* = 2R/\Delta t^*$. Noting that V_{horiz}^* is the time derivative of R , and that $R(0) = 1350 \text{ ft}$, we get

$$R(t) = 1350 \exp \left(\frac{-2}{\Delta t^*} t \right) \quad (9)$$

Substituting Eq. (8) into Eq. (9), and comparing the resultant equation with Eq. (7) yields

$$h^* = 69.2 + \left(\frac{80.8 \sqrt{R/1350}}{430.8} \right) \frac{1}{(\ln \sqrt{R/1350}) - 1} \quad (10)$$

The altitude rate along the reference trajectory is given by Eq. (6). For the general case in which the vehicle is not on the reference trajectory, that is, $h \neq h^*$, the vertical speed guidance law is of the

form $\dot{h}^G = \dot{h}^* + K_h(h^* - h)$, where h is the actual altitude and $K_h > 0$ is a feedback gain. Hence, the vertical speed guidance command is given by

$$\dot{h}^G = (-0.03714h^* + 2.57) + \left(\frac{h^* - h}{\tau} \right) \quad (11)$$

where $\tau = 1/K_h = 25$ s and h^* is obtained from Eq. (10). \dot{h}^G is set to a constant value of -3 fps when h first drops below 150 ft. To limit the effect of large altitude errors, the value of \dot{h}^G obtained from Eq. (11) is bounded by 0 and -30 fps.

Substituting Eq. (8) into the equation $V_{\text{horiz}}^* = 2R/\Delta t^*$, and then substituting Eq. (10) into the resulting equation yields the following relationship along the reference trajectory:

$$V_{\text{horiz}}^* = 0.04444R(1 - 0.5 \ln(R/1350)) \quad (12)$$

Let V_N^* and V_E^* denote lunar north and east components of the horizontal speed V_{horiz}^* , respectively, along the reference trajectory. Also, let x and y denote lunar north and east components, respectively, of the vehicle's range from the landing site, that is, $R = \sqrt{x^2 + y^2}$. Then,

$$V_N^* = 0.04444x(\ln \sqrt{R/1350} - 1) \quad (13a)$$

$$V_E^* = 0.04444y(\ln \sqrt{R/1350} - 1) \quad (13b)$$

For numerical conditioning, V_N^* and V_E^* are set to zero if $R < 0.1$ ft.

Transforming these guidance velocity components from lunar-surface-fixed axes to vehicle body axes, and noting that the down velocity component $V_D = -\dot{h}$, yields

$$V_x^G = (\cos \theta \cos \psi)V_N^G + (\cos \theta \sin \psi)V_E^G + (\sin \theta)\dot{h}^G \quad (14a)$$

$$V_y^G = (\sin \phi \sin \theta \cos \psi - \cos \phi \sin \psi)V_N^G + (\sin \phi \sin \theta \sin \psi + \cos \phi \cos \psi)V_E^G - (\sin \phi \cos \theta)\dot{h}^G \quad (14b)$$

where V_x^G and V_y^G are guidance velocity components along the vehicle body x and y axes, respectively.

The lunar north and east components of acceleration along the reference trajectory can be determined from analytical differentiation of Eq. (13). For the general case in which the vehicle is not on the reference trajectory, that is, $V \neq V^G$, the acceleration guidance law has the form $a^G = a^* + K_V(V^* - V)$, where V is the actual velocity and $K_V > 0$ is a feedback gain. The north and east components of acceleration guidance are obtained as

$$a_N^G = \left\{ \frac{V_N V_N^*}{x} + \left(\frac{0.02222x\dot{R}}{R} \right) \right\} + \left(\frac{V_N^* - V_N}{\tau} \right) \quad (15a)$$

$$a_E^G = \left\{ \frac{V_E V_E^*}{y} + \left(\frac{0.02222y\dot{R}}{R} \right) \right\} + \left(\frac{V_E^* - V_E}{\tau} \right) \quad (15b)$$

where $\tau = 1/K_V = 8$ s. For numerical conditioning, a_N is set to zero if $|x|$ is less than 0.1 ft; a similar rule applies in the y dimension.

Noting that tilting the descent engine thrust force, T , creates an acceleration in the horizontal plane, we have

$$ma_N = -T(\cos \phi \sin \theta \cos \psi + \sin \phi \sin \psi) \quad (16a)$$

$$ma_E = -T(\cos \phi \sin \theta \sin \psi - \sin \phi \cos \psi) \quad (16b)$$

The guidance roll and pitch angles, ϕ^G and θ^G , are determined from Eqs. (16a) and (16b):

$$\phi^G = \sin^{-1} \left\{ \frac{-m}{T} (a_N^G \sin \psi - a_E^G \cos \psi) \right\} \quad (17a)$$

$$\theta^G = \sin^{-1} \left\{ \frac{-m}{T \cos \phi^G} (a_N^G \cos \psi + a_E^G \sin \psi) \right\} \quad (17b)$$

To limit the effect of large trajectory errors, the values of ϕ^G and θ^G are bounded by ± 45 deg.

For guidance purposes, the range R is considered as the independent variable. First, the value of h^* is computed from Eq. (10); this is the altitude at which the vehicle would be flying if it were on the reference trajectory at range R from the landing site. The vertical speed guidance can now be computed from Eq. (11). This enables computation of the horizontal velocity components from Eqs. (13) and (14). Finally, the guidance roll and pitch angles can be computed from Eq. (17).

Guidance cues are presented to the pilot as errors from the desired vehicle states. These errors are computed as the differences between the guidance roll/pitch angle given by Eq. (17) and the corresponding actual values, and the guidance velocity components along the vehicle body axes given by Eq. (14) and the corresponding actual values. Details on the display of these guidance cues are presented in the next section.

Simulation Environment

The experiment was conducted on the Vertical Motion Simulator (VMS) at the NASA Ames Research Center. The VMS is a large motion base simulator [33] that has been used for numerous handling qualities evaluations [34]. A 6 deg of freedom simulator motion was used for the experiment because the reference trajectory was quite dynamic, featuring significant translational accelerations (~ 3 ft/s²) and roll/pitch angular motion (~ 15 deg). Although not formally verified, it is believed that motion cues are important for the flying task in this experiment.

The Apollo Lunar Module pilot stations had a standing configuration to improve downward visibility and reduce vehicle mass by eliminating seats. One of the VMS interchangeable cabs was structurally modified to provide a similar cockpit configuration; see Fig. 6. The evaluation pilot occupied the left station; the right station was occupied by the experimenter during training runs but was unoccupied for data collection runs. At each pilot station, there was a three-axis RHC and a three-axis THC mounted on the right and left armrest, respectively. Twisting the THC toggled between the descent engine control modes of throttle increment and descent rate. Up/down motion of the THC adjusted the commanded value of the throttle increment or rate of descent, depending on the selected mode.

A simulated view of the lunar landscape was projected on a set of five noncollimating flat screen rear projection color displays. The designated landing site was depicted by a 50-ft-diam (15.2-m-diam) red circle enclosed by a slightly larger red square on the lunar surface. The image resolution was 1/4 pixel per arcmin, corresponding to approximately 20/80 visual acuity. The display had a very large field of view: 77 deg vertical and 225 deg horizontal. Window masking was not used in the simulator cockpit; therefore, the entire field of view was available to the pilot. This is not representative of actual operations in which the pilots have only limited views of the lunar landscape through small windows. However, the precision landing task in this experiment was essentially a head-down task, and the pilot's attention was focused primarily on the cockpit instrumentation rather than the view outside the cockpit. This was true for guidance-on as well as guidance-off experiment configurations, but perhaps less so in the latter case.

Cockpit Instrumentation

Cockpit displays were mounted on a console providing two 9 in. flat panel monitors at each pilot station and a 15 in. flat panel monitor in the center. The pilot station displays are shown in Fig. 7; the center monitor displayed color-coded touchdown performance parameters given in Fig. 3 at the end of each run.

The left display has a "moving map" section with a triangle in the center representing the spacecraft; the dark circle indicates the landing site. The rings indicate range from the spacecraft's current

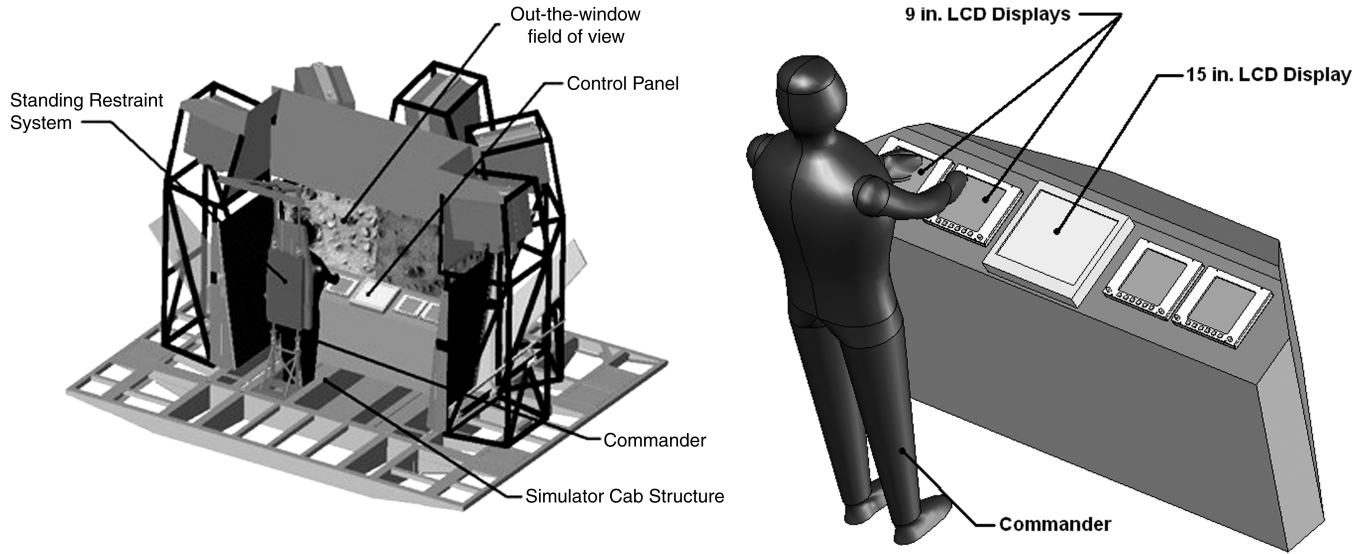


Fig. 6 Simulator cockpit layout.

location, and the radial lines indicate bearing angles in increments of 30 deg. The map rescales (zooms in) as the spacecraft approaches the landing site. The diamonds on the map section indicate the body x - and y -axis components of the vehicle's speed (fps). The bars on the map section are speed error needles that provide guidance for the vehicle's longitudinal and lateral speeds. This guidance is "fly to," which means that in the illustration of Fig. 7 the pilot should move the THC forward and right to drive the error needles to zero; however, it is noted that THC inputs are effective only when the vehicle is in a near-level attitude in the vicinity of the landing site. For experiment configurations with guidance off, both needles were locked at zero. Immediately below the moving map are digital readouts of range to go as well as its x (downrange) and y (cross range) components in units of feet. Next to the map section are thrust indicators and gauges showing propellant mass available for the main descent engine and the RCS jets.

The right display shows an attitude director indicator (ADI) with a digital readout of the roll, pitch, and yaw angles. The small triangles on the scales around the ADI indicate the body roll, pitch, and yaw rates; each tick mark on the scale is 5 deg/s. The bars on the ADI are attitude error needles that provide guidance for roll, pitch, and yaw angles. This guidance is "fly to," which means that in the illustration of Fig. 7 the pilot should use the RHC to roll right, pitch down, and

yaw right to drive the error needles to zero. In the experiment, the yaw guidance was turned off (yaw needle locked at zero) and pilots were advised not to make any yaw-axis RHC inputs because it added significant workload while adding little value to the flying task. However, the yaw attitude hold function was always active to null any yaw disturbances. For experiment configurations with guidance off, all three needles were locked at zero. On the lower right of the ADI is an annunciator for the throttle mode (throttle increment or descent rate) and the current commanded value for the selected mode. To the right of the ADI are three moving tape displays for horizontal speed (fps), altitude (ft), and altitude rate (fps).

Piloting Technique

The following procedures were presented to, and discussed with, each pilot during the initial briefing. The pilots practiced these procedures during the training and familiarization simulator session before data collection.

Vertical Speed Control

This is accomplished by manual or automatic control of the descent engine throttle setting. The small triangle on the right side of the altitude-rate tape in Fig. 7 is the vertical speed guidance

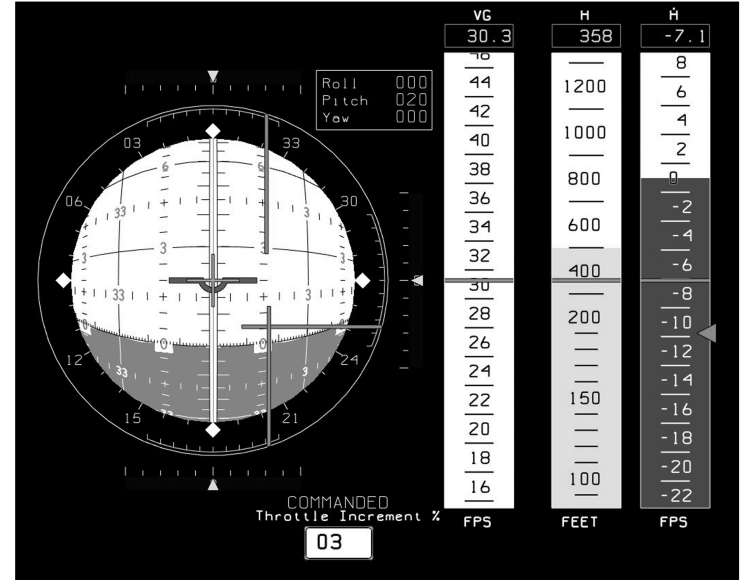
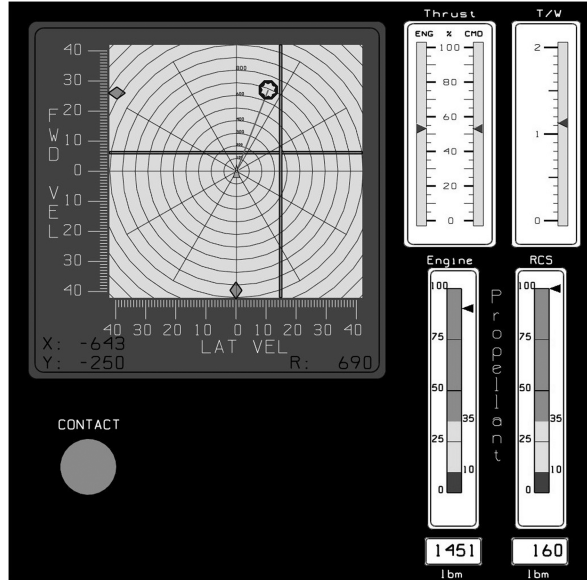


Fig. 7 Pilot station displays.

command. However, early testing indicated that manually changing the throttle setting to follow the vertical speed guidance command added substantially to the already-high pilot workload for speed control in the horizontal plane. In this experiment, a simpler technique was used to approximate the descent rate profile of the reference trajectory. The simulation began in throttle increment mode with a ΔT_{cmd} setting of 3% that had the effect of reducing the descent rate from an initial value of 16 fps at 500 ft altitude to 3 fps at approximately 150 ft altitude in the vicinity of the landing site. Pilots were advised to switch to rate-of-descent mode (by twisting the THC) at this point, and if necessary adjust the descent rate to 3 fps with up/down inputs from the THC.

Horizontal Speed Control with Guidance On

This is accomplished by rolling and/or pitching the vehicle to tilt the descent engine thrust vector. Pilots were advised to follow guidance commands by first using the RHC to null the roll/pitch angle error needles on the ADI until the vehicle reached a near-level attitude in the vicinity of the landing site, and then using the THC to null the forward/lateral speed error needles on the map display until touchdown. However, it was possible to fly the vehicle all the way to touchdown using only the RHC, by nulling error needles on the ADI to follow attitude guidance.

Horizontal Speed Control with Guidance Off

Pilots were asked to develop their own control techniques for the precision landing task. The error needles for attitude guidance and horizontal speed guidance were locked out at zero, but all other instrumentation was available. An out-the-window simulated view of the lunar landscape was available, as described earlier in this section.

Results

The axes of the experiment matrix were control power and guidance cues. There were six values of control power ranging from 100 to 15% of the nominal (Apollo) value. In the simulation model, control power was changed by simply scaling the value of RCS jet thrust. This resulted in appropriately scaled values of forces commanded by THC inputs and moments resulting from RHC inputs. It is noted that values of nominal angular accelerations (α) in the attitude-control laws of Eq. (5) were also appropriately scaled.

This section provides a detailed analysis of the experiment data. There were a total of 180 data collection runs: 108 for the guidance-on configurations and 72 for the guidance-off configurations, as described below.

Guidance On

Data were collected from six pilots for six values of control power ranging from 100 to 15% of the nominal value. The trajectory profile was described in the section on experiment design; it is noted that there is a left offset of 250 ft at the initial condition. Pilots were generally able to follow the guidance commands without much

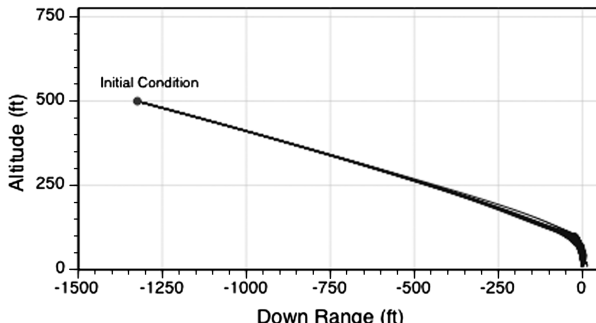


Fig. 8 Longitudinal trajectory profiles for offset approach with guidance on at 100% control power.

difficulty. Figure 8 shows the actual trajectory profiles flown by the six pilots (three data runs each) for the 100% control power configuration. Note that all 18 trajectory profiles are orderly and bunched closely together.

Handling Qualities Ratings

Figure 9 shows the handling qualities ratings, on the Cooper-Harper scale, of all six pilots for each of the six control powers, that is, 36 data points. In this bubble chart, the size of the bubble for a rating value indicates the number of pilots who assigned that rating. A star symbol indicates the median rating at each control power. For 100% control power, the handling qualities ratings are essentially Level 1, and for 50% control power the ratings are distributed across the Level 1–2 boundary. For 30% control power, the handling qualities ratings are essentially Level 2 and there are no Level 3 ratings. For 25% control power, half of the ratings are Level 3. This is indicative of a handling qualities “cliff” between 25 and 30% control power. For lower control powers (20 and 15%), the handling qualities ratings are distributed across the Level 2–3 boundary, and there are no Level 1 ratings.

The data in Fig. 9 exhibit some outliers that merit discussion. The rating of 9 at 15% control power was assigned because adequate performance could not be achieved (this requires a rating of 8 or worse). In the first two data runs, the range at touchdown was close to the limit of 15 ft; in the third run the range was 23 ft and the vehicle was almost out of descent engine propellant because there was a lot of back-and-forth maneuvering that almost doubled the nominal flying time. The ratings of 3 for the 25 and 30% control power configurations came from a pilot who consistently gave better ratings than the other five pilots. The rating of 4 for the 100% control power configuration came from a pilot who mostly gave worse ratings than the other five pilots.

Task Load Index Ratings

Figure 10 shows task load index (TLX) component ratings (averaged across six pilots) for selected control powers: 15, 50, and 100%. It is recalled that the six TLX components are mental demand, physical demand, temporal demand, performance, effort, and frustration. The TLX component ratings were assigned by pilots on a scale of 1–10, and were converted to a scale of 0–100 in post-processing. It can be seen from Fig. 10 that each component rating increases as control power decreases, with small changes across 100–50% control powers and large changes across 50–15% control powers. The data also indicate that the primary TLX components for this flying task are mental demand, temporal demand, and effort, whereas the secondary components are physical demand, performance, and frustration.

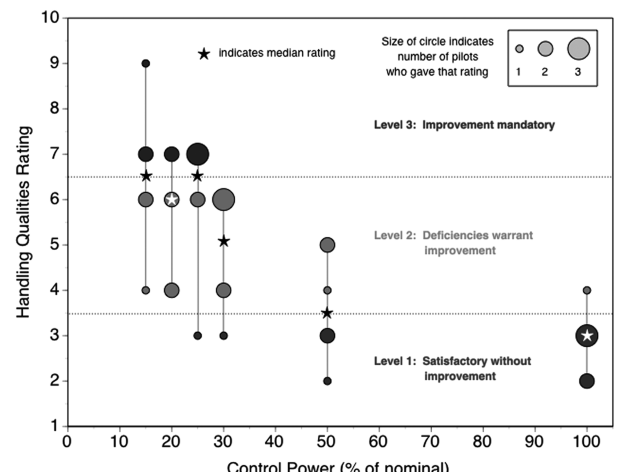


Fig. 9 Handling qualities rating vs control power for offset approach with guidance on.

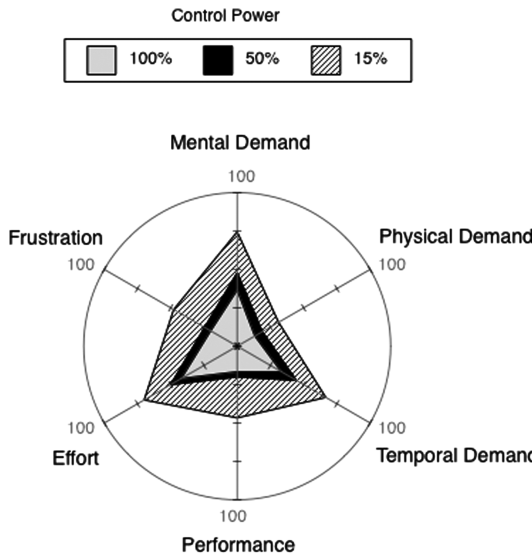


Fig. 10 Task load index component ratings for offset approach with guidance on.

Touchdown Performance

There were 10 parameters for touchdown performance; see Fig. 3 for a listing of these parameters and the corresponding limits for adequate performance. Data analysis revealed that adequate performance was generally achieved for all performance parameters. For example, Fig. 11 shows the dispersions of touchdown range (distance from center of landing pad) along with the limits of adequate performance shown by large circles, for 100 and 15% control powers. The 18 data points cover three runs for each of the six pilots. The median touchdown range for 100% control power was 1.7 ft (0.5 m) compared to 7.8 ft (2.4 m) for 15% control power, indicating that touchdown performance degrades as control power decreases.

Propellant Usage

It was observed that the RCS propellant usage decreased with control power; this is as expected because the RCS jets are scaled down as control power decreases. As noted earlier, handling qualities degrade as control power decreases. The relationship between RCS propellant usage and handling qualities ratings (parameterized by control power) was found to be almost linear, indicating that there is no optimum in that tradeoff.

Guidance Off

The original experiment plan was to evaluate handling qualities for the offset approach flying task across various control powers, with and without guidance. This would have permitted a direct comparison of handling qualities, at each control power, for guidance on vs off. However, it was found that the offset approach precision landing task was extremely difficult to fly without guidance, even for pilots with significant flying skills and experience. Within the

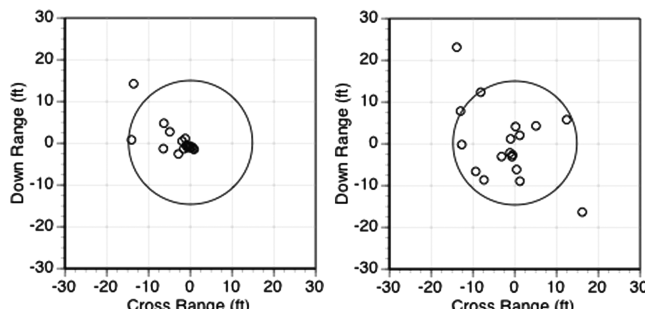


Fig. 11 Touchdown range for offset approach with guidance on:
a) 100% control power, and b) 15% control power.

constraints of limited time available for training and familiarization, none of the pilots was able to develop a good technique to consistently fly the offset approach with guidance off. However, they were able to develop their own techniques to fly a centerline (zero lateral offset) approach with guidance off; the techniques often involved designing a series of “gates” at various altitudes and associating them with target values of horizontal speed.

Because of schedule and other constraints, experiment data with guidance off were collected from four of the six evaluation pilots. Data were collected from these pilots for six values of control power ranging from 100 to 15% of the nominal value. The trajectory profile was described in the section on experiment design; it is noted that there is no lateral offset at the initial condition. Figure 12 shows the actual trajectory profiles flown by the four pilots (three data runs each) for the 100% control power configuration. Note that many of the 12 trajectory profiles are disorderly and show significant variations.

Results for the guidance-off case are presented with an important caveat: they cannot be directly compared with corresponding configurations for guidance on because the flying tasks are very different. Flying the offset approach with guidance on is a two-axis control task, whereas flying the centerline approach with guidance off is a one-axis task. Even within the guidance-off configurations, the data variability across pilots may be significant because each pilot developed his own flying technique.

Handling Qualities Ratings

Figure 13 shows the handling qualities ratings, on the Cooper-Harper scale, of all four pilots for each of the six control powers, that is, 24 data points. In this bubble chart, the size of the bubble for a rating value indicates the number of pilots who assigned that rating. A star symbol indicates the median rating at each control power. For 100% control power the handling qualities ratings are all Level 1,

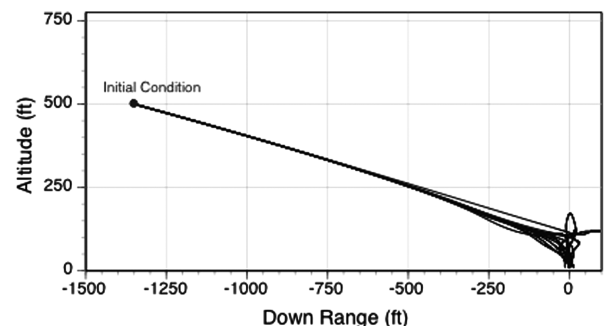


Fig. 12 Longitudinal trajectory profiles for centerline approach with guidance off at 100% control power.

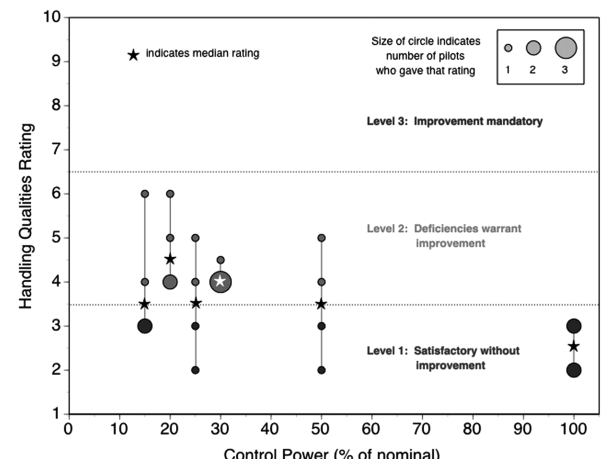


Fig. 13 Handling qualities rating vs control power for centerline approach with guidance off.

and for 50% control power the ratings are evenly distributed across the Level 1–2 boundary. For lower control powers (30–15%) the handling qualities ratings do not exhibit a clear trend. It is noted that there are no Level 3 ratings.

Task Load Index Ratings

Figure 14 shows TLX component ratings (averaged across four pilots) for selected control powers: 15, 50, and 100%. It is recalled that the six TLX components are mental demand, physical demand, temporal demand, performance, effort, and frustration. The TLX component ratings were assigned by pilots on a scale of 1–10, and were converted to a scale of 0–100 in postprocessing. It can be seen from Fig. 14 that each component rating increases as control power decreases, with significant changes across the control powers. The data also indicate that the primary TLX components for this flying task are mental demand, temporal demand, and effort, whereas the secondary components are physical demand, performance, and frustration.

Touchdown Performance

There were 10 parameters for touchdown performance; see Fig. 3 for a listing of these parameters and the corresponding limits for adequate performance. Data analysis revealed that adequate performance was generally achieved for all performance parameters. For example, Fig. 15 shows the dispersions of touchdown range (distance from center of landing pad) along with the limits of adequate performance shown by large circles, for 100 and 15% control powers. The 12 data points cover three runs for each of the

four pilots. The median touchdown range for 100% control power was 1.7 ft (0.5 m) compared to 6.2 ft (1.9 m) for 15% control power, indicating that touchdown performance degrades as control power decreases.

Conclusions

An evaluation of lunar lander handling qualities was conducted by six pilot astronauts flying the NASA Ames Research Center VMS. The objective was to study the effects of control power and guidance cues on handling qualities for a precision landing task from final approach through terminal descent to touchdown.

For a lateral offset approach with guidance on, the handling qualities degraded nonlinearly as control power decreased. For 100% control power the handling qualities ratings were essentially Level 1, and for 50% control power the ratings were distributed across the Level 1–2 boundary. For 30% control power the handling qualities ratings were essentially Level 2, but for 25% control power half of the ratings were Level 3. This is indicative of a handling qualities cliff between 25 and 30% control power. The TLX component ratings increased with control power, and the primary factors for this flying task were found to be mental demand, temporal demand, and effort. Adequate performance was generally achieved for all performance parameters. For touchdown range, the median value for 100% control power was 1.7 ft compared to 7.8 ft for 15% control power, indicating that touchdown performance degrades as control power decreases.

The task of precision landing from offset approach was extremely difficult to fly without guidance, even for pilots with significant flying skills and experience. Within the constraints of limited time available for training and familiarization, none of the pilots was able to develop a good technique to consistently fly the offset approach with guidance off. However, they were able to develop their own techniques to fly a centerline (zero lateral offset) approach with guidance off; the techniques often involved designing a series of gates at various altitudes and associating them with target values of horizontal speed. For 100% control power, the handling qualities ratings were all Level 1, and for 50% control power the ratings were evenly distributed across the Level 1–2 boundary. For lower control powers (30–15%) there was no clear trend in handling qualities ratings, but there were no Level 3 ratings. The TLX component ratings increased with control power, and the primary factors for this flying task were found to be mental demand, temporal demand, and effort. Adequate performance was generally achieved for all performance parameters. For touchdown range, the median value for 100% control power was 1.7 ft compared to 6.2 ft for 15% control power, indicating that touchdown performance degrades as control power decreases.

This initial experiment demonstrates that a precision landing requirement adds substantial difficulty to the already challenging flying task from final approach to lunar touchdown. The results clearly establish the need for good handling qualities in terms of control power requirements, as well as the need for appropriate guidance cues.

Acknowledgments

The efforts of the Simulation Laboratories staff at NASA Ames Research Center are greatly appreciated. In particular, the author would like to acknowledge the substantial contributions of Mike Weinstein, who developed all software for the lunar lander dynamics/control model and also served as simulation engineer for the experiment. Bo Bobko served as project pilot and contributed to model development and testing. Boris Rabin created the lunar landscape graphics for the cockpit window displays. Steve Beard provided simulator cab graphics for Fig. 6. Thanks are due to Chad Frost, Eric Mueller, and Fraser Thomson of NASA Ames Research Center for discussions on experiment design, assistance with data collection, and assistance with postprocessing, respectively. Eric Boe from NASA Johnson Space Center served as liaison with the Crew Office and provided valuable feedback during the development and testing phase of this effort.

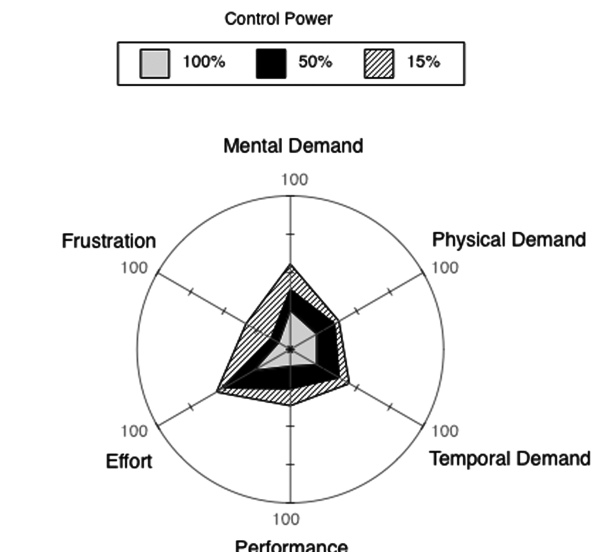


Fig. 14 Task load index component ratings for centerline approach with guidance off.

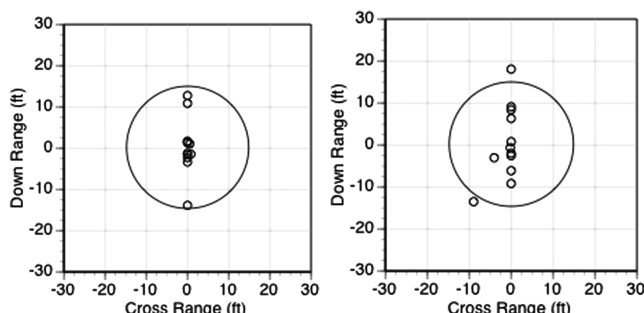


Fig. 15 Touchdown range for centerline approach with guidance off:
a) 100% control power, and b) 15% control power.

References

- [1] Cooper, G. E., and Harper, R. P., "The Use of Pilot Rating in the Evaluation of Aircraft Handling Qualities," NASA TN D-5153, April 1969.
- [2] Soulé, H. A., "Preliminary Investigation of the Flying Qualities of Airplanes," NACA TR 700, 1940.
- [3] Gilruth, R. R., "Requirements for Satisfactory Flying Qualities of Airplanes," NACA TR 755, 1941.
- [4] Harper, R. P., and Cooper, G. E., "Handling Qualities and Pilot Evaluation," *Journal of Guidance, Control, and Dynamics*, Vol. 9, No. 5, Sept.–Oct. 1986, pp. 515–529.
doi:10.2514/3.20142
- [5] Phillips, W. H., "Flying Qualities from Early Airplanes to the Space Shuttle," *Journal of Guidance, Control, and Dynamics*, Vol. 12, No. 4, 1989, pp. 449–459.
doi:10.2514/3.20432
- [6] Mitchell, D. G., Doman, D. B., Key, D. L., Klyde, D. H., Leggett, D. B., Moorhouse, D. J., Mason, D. H., Raney, D. L., and Schmidt, D. K., "Evolution, Revolution, and Challenges of Handling Qualities," *Journal of Guidance, Control, and Dynamics*, Vol. 27, No. 1, 2004, pp. 12–28.
doi:10.2514/1.3252
- [7] "Military Specification, Flying Qualities of Piloted Airplanes," U.S. Air Force, MIL-F-8785C, Wright-Patterson Air Force Base, OH, Nov. 1980.
- [8] "Aeronautical Design Standard, Performance Specification: Handling Qualities Requirements for Military Rotorcraft," U.S. Army—Aviation and Missile Command, ADS-33E-PRF, Redstone Arsenal, AL, March 2000.
- [9] Powers, B. G., "Space Shuttle Longitudinal Landing Flying Qualities," *Journal of Guidance, Control, and Dynamics*, Vol. 9, No. 5, Sept.–Oct. 1986, pp. 566–572.
doi:10.2514/3.20147
- [10] Besco, R. O., "Handling Qualities Criteria for Manned Spacecraft Attitude-Control Systems," *Journal of Spacecraft and Rockets*, Vol. 2, No. 4, July–Aug. 1965, pp. 628–630.
doi:10.2514/3.28252
- [11] Matranga, G. J., Washington, H. P., Chenoweth, P. L., and Young, W. R., "Handling Qualities and Trajectory Requirements for Terminal Lunar Landing, as Determined from Analog Simulation," NASA TN D-1921, Aug. 1963.
- [12] Cheatham, D. C., and Hackler, C. T., "Handling Qualities for Pilot Control of Apollo Lunar-Landing Spacecraft," *Journal of Spacecraft and Rockets*, Vol. 3, No. 5, May 1966, pp. 632–638.
doi:10.2514/3.28506
- [13] Matranga, G. J., Mallick, D. L., and Kluever, E. E., "An Assessment of Ground and Flight Simulators for the Examination of Manned Lunar Landing," AIAA Paper 67-238, 1967.
- [14] Hewes, D. E., "Interim Report on Flight Evaluations of Lunar Landing Vehicle Attitude Control Systems," AIAA Paper 67-239, 1967.
- [15] Goode, M. W., and Person, L. H., "Flight Test Evaluation of a Small One-Man Lunar Flying Device," *Journal of Spacecraft and Rockets*, Vol. 5, No. 12, 1968, pp. 1468–1472.
doi:10.2514/3.29504
- [16] Anon., "Lunar Landing Research Vehicle: Estimated Handling Qualities," Bell Aerosystems Co. Rept. 7161-954004, (NASA CR-127487), April 1964.
- [17] Kluever, E. E., Mallick, D. L., and Matranga, G. J., "Flight Results with a Non-Aerodynamic, Variable Stability, Flying Platform," Society of Experimental Test Pilots, Paper 1333, 1966.
- [18] Jarvis, C. R., "Fly-by-Wire Flight Control System Experience with a Free-Flight Lunar-Landing Research Vehicle," AIAA Paper 67-273, 1967.
- [19] Jarvis, C. R., "Flight Test Evaluation of an On-Off Rate Command Attitude Control System of a Manned Lunar-Landing Research Vehicle," NASA TN D-3903, April 1967.
- [20] Hackler, C. T., Brickel, J. R., Smith, H. E., and Cheatham, D. C., "Lunar Module Pilot Control Considerations," NASA TN D-4131, Feb. 1968.
- [21] O'Bryan, T. C., and Hewes, D. E., "Operational Features of the Langley Lunar Landing Research Facility," NASA TN D-3828, Feb. 1967.
- [22] Bellman, D. R., and Matranga, G. J., "Design and Operational Characteristics of a Lunar-Landing Research Vehicle," NASA TN D-3023, Sept. 1965.
- [23] NASA's Exploration Systems Architecture Study, NASA TM-2005-214062, Nov. 2005.
- [24] Sim, L., Cummings, M. L., and Smith, C. A., "Past, Present and Future Implications of Human Supervisory Control in Space Missions," *Acta Astronautica*, Vol. 62, 2008, pp. 648–655.
doi:10.1016/j.actaastro.2008.01.029
- [25] Anon., "Human-Rating Requirements for Space Flight Systems," NASA Procedural Requirements, NPR 8705.2B, May 2008, pp. 34–35.
- [26] Mueller, E. R., Bilimoria, K. D., and Frost, C. F., "Initial Handling Qualities Evaluation for Spacecraft Docking in Low Earth Orbit," AIAA Paper 2008-6832, Aug. 2008.
- [27] Bailey, R. E., Jackson, E. B., and Goodrich, K. H., "Initial Investigation of Reaction Control System Design on Spacecraft Handling Qualities for Earth Orbit Docking," AIAA Paper 2008-6553, Aug. 2008.
- [28] Hart, S. G., and Staveland, L. E., "Development of NASA-TLX (Task Load Index): Results of Empirical and Theoretical Research," *Human Mental Workload*, edited by P. A. Hancock and N. Meshkati, North Holland Press, Amsterdam, The Netherlands, 1988, pp. 139–183.
- [29] Donahue, B. B., Caplin, G. N., and Smith, D. B., "Lunar Lander Concept Design for the 2019 NASA Outpost Mission," AIAA Paper 2007-6175, Sept. 2007.
- [30] Shelton, D. H., "Apollo Experience Report—Guidance and Control Systems: Lunar Module Stabilization and Control System," NASA TN D-8086, Nov. 1975.
- [31] Stengel, R. F., "Manual Attitude Control of the Lunar Module," *Journal of Spacecraft and Rockets*, Vol. 7, No. 8, Aug. 1970, pp. 941–948.
doi:10.2514/3.30075
- [32] Widnall, W. S., "Lunar Module Digital Autopilot," *Journal of Spacecraft and Rockets*, Vol. 8, No. 1, Jan. 1971, pp. 56–62.
doi:10.2514/3.30217
- [33] Danek, G. L., "Vertical Motion Simulator Familiarization Guide," NASA TM 103923, May 1993.
- [34] Aponso, B. L., Tran, D. T., and Schroeder, J. A., "Rotorcraft Research at the NASA Vertical Motion Simulator," AIAA Paper 2009-6065, Aug. 2008.

D. Spencer
Associate Editor